1995

Building a Continuous Wave Titanium Sapphire Laser

Sean McClain
College of Saint Benedict/Saint John's University

Building a Continuous Wave Titanium Sapphire Laser

A THESIS
The Honors Program
College of St. Benedict/St. John's University

In Partial Fulfillment
of the Requirements for the distinction "All College Honors"
and the Degree Bachelor of Arts
in the Department of Physics

by
Sean Thomas McClain
May 26, 1995

Building A Continuous Wave Ti:Sapphire Laser

Sean Thomas McClain

May 26, 1995

Abstract

In fulfilling the requirement of a senior thesis, I have constructed and optimized a continuous wave (cw) titanium sapphire laser, loosely based on the designs of other experimenters. A maximum output power of 500 mW at 794 nm was obtained after trying several cavity configurations. The beam characteristics, including wavelength, beam width, power and position stability were found to be sensitively dependent on the pump power, supplied by an argon-ion laser.

I.Introduction

Since its first reported room temperature use in 1986,[1] cw titanium sapphire lasers have become both easier to produce and to use. In spite of their increasing popularity, building one's own Ti:sapphire laser is still very much a trial and error process. Over the course of the past year I built and studied a cw Ti:sapphire laser, loosely modeled after designs give by M.M. Murnane et al.[2] . While building the laser, different cavities and components were tried in an attempt to improve upon previous designs.

As background for the construction of a Ti:sapphire laser, Section II reviews the general theory of lasers, and Section III gives a more in depth look at the theory of laser operation as it pertains to the Ti:sapphire.

II.General Laser Theory

Despite the large variety in laser designs and construction, at the heart of all laser technology lies three basic principals. Taken together, these three principles (spontaneous emission, stimulated emission, and stimulated absorption) form the basis of how light interacts with the material world.

To describe the processes of stimulated absorption and emission, one must look at what is happening at the atomic level. As an example, consider the case of an atom containing an electron in its ground state (E_0), being struck by a photon of frequency ν. When the photon collides with the electron, it imparts to it an energy

$$h\nu = E_1 - E_0 \tag{1}$$

where h is Planck's constant and E_1 is an excited energy state. This process of the atom absorbing the photon is the stimulated absorption alluded to above. There are restrictions on this process though. Since an electron may only occupy certain discrete energy levels, only a certain range of wavelengths may be absorbed, and some will be more easily absorbed than others. The range of wavelengths that are absorbed by a material are known as its absorption spectra.

After the photon excites the electron to a higher energy level, it may decay back to the ground state by one of two processes, stimulated or spontaneous emission. In spontaneous emission, an electron in an excited state spontaneously emits a photon with a random phase,

direction, and wavelength. As a result, the electron loses energy and decays to a lower state. In stimulated emission, a passing photon "stimulates" an electron in an excited state to emit a photon, which has the same phase, direction, and wavelength as the original photon.[3] As with spontaneous emission, the electron now loses energy, and decays to a lower energy level.

Regardless of the process taking place, all transitions of electrons between energy levels fall into one of two categories; they are either classified as being highly probable or highly improbable. A more quantitative approach to these transitions can be taken by using the transition lifetime (τ). The transition lifetime is a measurement of the time during which energy is emitted or absorbed during a transition. The highly improbable states then have a much longer τ, and are known as metastable states.[4]

The laser is capable of using the above three processes to produce a beam with a high degree of monochromaticity, coherence, and directionality. To produce such a beam, all lasers manipulate the three above processes with three main components: the pump, the lasing material, and the resonator.

In a laser, the pump serves as the source of energy required to induce stimulated absorption, while the lasing material serves as the deposit of electrons. The pump may be a chemical, thermal, electrical, or optical source, while the lasing material may be any collection of atoms, molecules, or ions that fluoresce when excited (Ref.4, 51).

In order for a laser to work, a large number of electrons must stay in a high energy state

long enough for the rate of stimulated emission to be greater than the rate of stimulated absorption (a condition known as a population inversion). For this to happen, lasers use either a two or four step pumping system. Both the two and four step systems first excite the electrons to a high energy state. The electrons then decay to a metastable state in a fast transition. Due to the metastable state's long τ, a population inversion occurs.

It is the final element of the laser, the resonator, that actually amplifies the emitted light and produces the output beam. When a population inversion occurs at the metastable level, the lasing material emits more photons than it is absorbing. The resonator then acts as an optical feedback device, reflecting emitted photons back and forth through the lasing material. Each new photon reflected in the resonator stimulates more emissions, which in turn stimulate even more photons, thus amplifying the beam.

As noted earlier, the linewidth of a laser's characteristic fluorescence spectrum is limited by the properties of its lasing material, but it is also affected by the characteristics of its resonator. Because the laser's cavity is basically a Fabry-Perot resonator, the wavelengths (λ) allowed are governed by the equation

$$\frac{m\lambda}{2} = L \tag{2}$$

where m is any integer and L is the length of the cavity.

III. Ti:Sapphire Theory

While the above discussion of how a laser works in general holds true for any laser, a Ti:sapphire laser does have some important differences. Following the order used in the general case, the theory of how the Ti:sapphire operates will first be looked at, followed by how its specific components function.

To begin with, in a Ti:sapphire laser, the lasing material consists of the host Al_2O_3 crystal and the active Ti_3^+ ion. The doping of the sapphire crystal with titanium results in one of the main distinctions between the Ti:sapphire and other solid-state lasers, that being its broad spectrum of lasing wavelengths. The emission spectra for a Ti:sapphire ranges from 660 to 1180 nm (Figure 1).[5] Such a large range of wavelengths was previously only approachable using dye lasers. Since the Ti:sapphire does have such a large fluorescence curve, the output beam is easily tunable over a wide range of wavelengths. Also noticeable in Figure 1 is that the Ti:sapphire has an absorption curve spanning 400 to 600 nm, and so it can easily be pumped by an argon-ion laser.

In addition to being tunable, another result of the Ti:sapphire's broad fluorescence curve is its ability to operate in a pulsed mode. If the various modes oscillating within the cavity are forced to maintain a fixed phase relative to one another, the resulting output will be pulsed, and the laser is said to be mode-locked (Ref.4, 120). Ti:sapphire lasers are capable of operating in a self-modelocked state, but at the present time the exact physics behind its

ability to do so are unknown. It is believed that the crystal's nonlinear index of refraction, coupled with a symmetric cavity, play a large role in self-modelocking.[6,7]

Since cavity design plays such an important role in mode-locking, Ti:sapphire resonators can be divided into two groups; symmetrical cavities for pulsed operation, and asymmetrical cavities for continuous wave. The asymmetrical arrangements are generally the simpler of the two.

The most basic cavity for cw operation is a linear cavity (Figure 2). In this setup, the two cavity mirrors are placed on axis to the incident pump beam. Both mirrors have a high transmission at 488-514 nm, and a high reflectance at the Ti:sapphire's 800 nm. With this cavity, none of the Ti:sapphire beam is let out of the cavity.

The second type of cw cavity is the V cavity (Figure 2), taken from an article by A. Sanchez (Ref.1). In this setup, the first cavity mirror is rotated off the pump beam axis to an output coupler. The advantage of this cavity is its relatively simple alignment while still allowing an output beam.

For working in a pulsed mode, there are two basic designs. The first of these is the ring cavity (Figure 2). In this setup, both cavity mirrors are turned off-axis to an output coupler. The second symmetrical cavity, the X (Figure 2), was taken from M. Murnane et al. (Ref.2) In this cavity, both cavity mirrors are rotated off axis.

IV.Construction

In building the Ti:sapphire laser, several different components and cavity designs were tried in an attempt to improve upon existing designs. In spite of this, many basic procedures and parts were used in each set up. While Section V will focus on the chronological list of each cavity and procedure tried, the following is a list of all components and procedures used in every cavity. Additional information on each part can be found in Table 1.

The Ti:sapphire was a 5 x 8 mm crystal, with a 4.75 mm path length and .15% doping. The ends of the crystal were cut at the Brewster angle.

The two cavity mirrors used are highly reflective at 800 nm, highly transmissive at 488-514 nm, and have a 10 cm radius of curvature.

In all cavities cooling of the crystal was accomplished by setting it on an aluminum prism mount, and by clamping it in place with an aluminum rod. Water and thermo-electric chips were initially considered, but it was found that other experiments had used up to 9 W of pump power and no cooling, with no adverse affects to the crystal.[8]

A Soliel-Babinet compensator was originally used to rotate the argon beam's polarization to match that of the crystal. However, this arrangement proved too easy to accidentally knock out of place, and so it was replaced by a pair of mirrors at 45° to the table, with one positioned over the other.

To insure maximum transmittance, it is important to orient the normal to the crystal's

face at the Brewster angle to the beam. The Brewster angle is found using the equation

$$\theta_B = \arctan \frac{n_c}{n_{air}} \tag{3}$$

where n_{air} is 1, and for sapphire at 786 nm n_c is 1.7606. Using Eq.4, the Brewster angle is found to be 60.4°. To position the normal to the crystal's face at this angle to the beam, a Coherent 200 power meter was used. At the Brewster angle, the amount of the pump beam being reflected from the crystal is at a minimum (ie. maximum transmission), and therefore the Brewster angle can be found by rotating the crystal until the reflected beam power is a minimum.

To insure that the maximum amount of pump power was being applied to the active area in the crystal, a plano-convex mirror was set outside the cavity, with its focus centered at the crystal. The reduced width of the focused pump beam allowed a much higher power per unit area (irradiance) than would have otherwise been possible.

In all cavity designs the two cavity mirrors, the crystal and prism table were mounted on a rail and carriage system. The lens was mounted directly outside the cavity, in front of the first cavity mirror. All components were mounted 14.5 cm off the table, parallel to it.

V.Experimentation

The first cavity design attempted was a cw linear setup, using only the two cavity mirrors and no output mirror (Figure 3). A plano-convex lens with a focal length of 25 cm was used to focus the pump beam in the crystal. The Soliel-Babinet compensator was used to

rotate the pump beam's polarization. Lasing was never observed with this cavity. The most probable reason why the linear cavity did not work was the low pump power. The lens used was absorbing a great deal of the pump beam (about .6 W), leaving only 3 W of pump power at the crystal. A minimum of 5 W of pump power at the crystal is recommended for the initial alignment of any cavity (Ref.2).

The second cavity tried was the ring cavity (Figure 4). The off-axis mirror used was a flat, silvered mirror. The same lens and polarization rotator were used in this set-up as in the linear cavity. Consequentially, this cavity was plagued by the same problems as the first. In addition to low pump power, the ring cavity also was very difficult to align. All three mirrors must be aligned together, due to their interdependent set-up. The rail and carriage design was not stable enough to allow such precise alignment. Due to these problems, lasing was never observed with this cavity.

The third resonator set-up was an X cavity (Figure 5). Before trying this design, the argon-ion laser was serviced by a Coherent technician, bringing the laser's maximum power up to 6 W. The two 45° mirrors were substituted for the Soliel-Babinet compensator, and a new lens with a 15 cm focal length was used. The two end mirrors were both flat, silvered mirrors. The result of the new lens and repaired argon-ion laser was a pump power of 5.2 W at the crystal, but lasing was still not observed. The most probable reason for this was the difficulty in aligning the X cavity.

The last cavity tried was the V cavity (Figure 6). A new top mirror was put in the polarization rotator for this cavity, resulting in a .6 W gain in pump power at the crystal, giving a total of 5.8 W. In addition to the new polarization rotator mirror, a partially reflective output coupler was purchased to replace the silvered mirrors previously used. The new output coupler was 90% reflective (at 800 nm), and thus allowed the Ti:sapphire out of the cavity for the first time. This cavity was exceptionally easy to align and work with. As a result of its ease of alignment, lasing was observed with this cavity.

VI.Alignment Procedure

For the V cavity, alignment proved to be straightforward. The off-axis cavity mirror was rotated to the smallest angle possible, to avoid astigmatism. The smallest angle attainable with this setup, while still avoiding all other components, was 10°. To position the three mirrors, I made use of the lens equation

$$\frac{1}{f} = \frac{1}{i} + \frac{1}{o} \tag{4}$$

where f is the focal length, i is the image distance, and o is the object distance. For the mirrors to be aligned, each should focus the crystal's light back to its center. This image is then used as the object for the other mirror. For the second cavity mirror then, the object and image distance must be equal. Using Eq. 4, with f equaling the mirror's 5 cm focal length, the image distance must equal 10 cm.

For the first cavity mirror, the reflected Ti:sapphire light is first being sent to the flat output coupler, then back to the mirror to be focused at the crystal. If the first cavity mirror is placed its focal length (5 cm) away from the crystal, then from Eq. 4 the image is formed at infinity (in essence forming a plane wave). The flat output coupler reflects the light back to the cavity mirror as a plane wave, which is then focused at the center of the crystal.

In practice, all of the alignment was a trial and error process. No accurate method of measuring cavity dimensions was found, so all measurements are only approximate. After much experimentation, a reliable method for getting the Ti:sapphire to lase was discovered.

To begin with, the crystal was positioned at the focus of the lens. This position was guessed by looking for the narrowest section of the pump beam. Once the crystal was in place, a piece of paper was placed in the path of the ray reflected from the first cavity mirror, at the greatest distance away possible. The first cavity mirror was then moved on the rail until the smallest fluorescence spot was observed on the piece of paper. The reasoning behind this is that at the smallest fluorescence spot size, the mirror is focusing the light on the distant paper. Since the output coupler is going to be much closer to the first cavity mirror than the paper, the distance to the focus at the paper can be approximated as infinity. If the mirror is focusing at infinity, then the reflected light at the output coupler can be approximated as a plane wave. Therefore, when the smallest fluorescence spot size is observed, the first cavity mirror is aligned.

To align the second cavity mirror a similar technique was used. The second cavity mirror was first moved on the rail until its fluorescence spot was at a minimum on the same piece of paper. Once the correct distance was found, the angle of the mirror was rotated until its fluorescence spot overlaid the fluorescence spot of the first mirror. When the two spots were directly on top of each other, the mirrors were correctly aligned.

The last step in the alignment procedure consisted of positioning the output coupler. No relation was ever found between the Ti:sapphire's ability to lase and the distance from the first cavity mirror and the output coupler, except that it must be less than the focus distance of the first cavity mirror. As long as the mirror was at the correct angle, the distance separating the two seemed to have no effect. After choosing an arbitrary distance to place the output coupler at, it was rotated back and forth. The correct angle, and hence lasing, was detected by a brief dimming in the crystal. This dimming is a consequence of the rate of stimulated emission surpassing that of spontaneous emission.

Once the Ti:sapphire was lasing, mirror positions and angles were varied in an attempt to find the maximum power output. A longpass filter was placed behind the output coupler to eliminate all pump beam radiation. The power was then checked with a Coherent power meter 200. The maximum Ti:sapphire power output was found to be 500 mW. The cavity dimensions at this power are shown in Figure 6. The distances do not correspond exactly to those predicted by Eq. 4 because of the effect of the light traveling through the crystal.

Likewise, the crystal is not exactly 12.5 cm from the lens because the lens' focal length is changed slightly by traveling through the first cavity mirror.

VII.Beam Analysis

Once the beam power was maximized, several characteristics of the Ti:sapphire laser were studied. Using a Burleigh Wavemeter Jr., the wavelength of the Ti:sapphire beam was found to be 794 nm. A beam scanner connected to a computer was then used to obtain data on the beam's power, change in position in the cavity, and width. The computer was also capable of fitting the beam's distribution to a Gaussian curve. Using the beam scanner, 1000 samples were taken at maximum output power. Each sample recorded the beam's position, width, and power. The results are shown in graph form in (Figure 7) and in chart form (Figure 8). From the data given in Figure 7, over the 1000 samples the width of the beam was found to vary by .5%, the power by 1.3%, and the position by .2%. The large standard deviations shown in Figure 7 and the variations shown in the graphs of Figure 8 attest to the beam's instability. In addition to the wavemeter and beam scanner, a Burleigh Spectrum Analyzer was used in an attempt to determine the bandwidth. However, the beam proved to be too unstable to get a usable reading.

The effects on the Ti:sapphire beam from varying the pump power were also studied. Using the Coherent power meter and the beam scanner, the Ti:sapphire's output power, change in position, and change in width were recorded over a range of input powers. The

power of the input beam was recorded before the lens, and the output power was recorded after the longpass filter (Figure 9). After all the data was taken, power readings were taken before the lens and at the crystal, in order to find a proportionality constant between the two. The input power was then multiplied by this constant to find the power at the crystal. A graph of the input power at the crystal versus the Ti:sapphire's output power is shown in Figure 10. The linear distribution of the data agrees with the results of previous experiments (Ref.1).

Graphs were also made of the Ti:sapphire beam's change in position and width at varying pump powers (Figures 11 and 12). The erratic nature of these graphs show once again the unstable nature of this laser.

Last of all, power readings taken were from directly before the crystal and directly after the crystal. The data gained from these power readings revealed the crystal's absorption (A) to be 77%. The data from the samples can be seen in Tables 2 and 3.

IX.Results

Utilizing the data found by varying the pump power, the theoretical and measured efficiencies of the Ti:sapphire beam can be calculated. The definition of efficiency used in in this case was

$$Efficiency = \frac{PowerOutput}{PowerInput}$$

The first term in this equation can be found by expressing the power input as

$$\frac{hc}{\lambda_p} \tag{5}$$

where λ_p is the pump laser's wavelength. The last term now needed to find the efficiency is the energy of the Ti:sapphire beam. Taking into account the transmission of the output coupler (T), the energy of the Ti:sapphire can be expressed as

$$T\frac{\lambda_p}{\lambda_l} \tag{6}$$

where λ_l is the Ti:sapphire's wavelength. The resultant equation for the theoretical efficiency η_Q is then found by dividing Eq.6 by Eq.5, giving

$$\eta_Q = T\frac{\lambda_p}{\lambda_l} \tag{7}$$

As a check of the theoretical efficiency, a measured efficiency was also calculated. Since the efficiency was earlier defined as the Ti:sapphire output power divided by the input pump power, the measured efficiency can be found from the slope of Figure 10. Using Eq.7, the theoretical and measured efficiencies were found to have values of 6% and 16%, respectively. The discrepancy between these two values can be explained by the difficulty of attaining accurate power reading of both the argon-ion and Ti:sapphire beams.

X.Conclusions

In conclusion, I was was able to build a cw Ti:sapphire laser with a maximum power output of 500 mW at 794 nm using a V cavity. The theoretical and measured efficiencies

were found to be 6% and 16%, respectively, with a crystal absorption of 77%. However, the resulting Ti:sapphire beam was found to be very unstable. At maximum power the width of the beam was found to vary by .5%, the power by 1.3%, and the position by .2%. The most probable cause for this instability was from the components used in building the cavity. The rail and carriage system was very susceptible to any vibrations or movement, and as a result was much too unstable to allow the precise horizontal control needed to align the mirrors. Mounting all the parts in a more stable system would probably improve the beam stability, and ease of use, immensely.

Acknowledgments

I would like to thank Dr. Dean Langley for all the help he gave me with this project. Without his unbelievable patience and hard work, this thesis would have never gotten past the planning stage.

I would also like to thank Dennis Myers. The help and encouragement he provided, along with part of his own time, finally got this project moving in a positive direction.

Project Title:
The Building of a Continuous Wave Titanium Sapphire Laser

Approved by:

Project Advisor, Associate Professor of Physics

Associate Professor of Physics

Associate Professor of Physics

Chair, Department of Physics

Directors, Honors Thesis Program

Director, Honors Program

References

1. A. Sanchez, R.E. Fahey, A.J. Strauss, and R.L. Aggarwal, "Room-temperature continuous-wave operation of a Ti:Al_2O_3 laser," Opt. Lett. **11**, 363-364 (1986).

2. M.M. Murnane, H.C. Kapteyn, C.P. Huang, M. Asaki, and D. Garvey, "Designs and guidelines for constructing a mode-locked ti:sapphire laser, Rev 1.6", 1992.

3. Frank L. Pedrotti S.J., and Leno S. Pedrotti, *Introduction to Optics* (Englewood Cliffs, New Jersey, 1993), 428.

4. Donald C. O'Shea, W. Russell Callen, and William T. Rhodes, *Introduction to Lasers and Their Applications* (Reading, Massachusetts, 1978) 54-55.

5. Peter F. Moulton, "Ti:sapphire lasers: Out of the lab and back in again," Optics and Photonics News, 20-23 (August, 1990).

6. Henry C. Kapteyn and Margaret M. Murnane, "Femtosecond Lasers: The Next Generation," Optics and Photonics News, 20-28 (March, 1994).

7. Margaret M. Murnane and Henry C. Kapteyn, "The Recent Revolution in Femtosecond Lasers," IEEE LEOS Newsletter, 17-19 (August, 1993).

8. C. Zimmermann, V. Vuletic, A. Hemmerich, L. Ricci, and T. W. Hänsh, "Design for a compact tunable Ti:sapphire laser," Opt. Lett. **20**, 297-299 (1995).

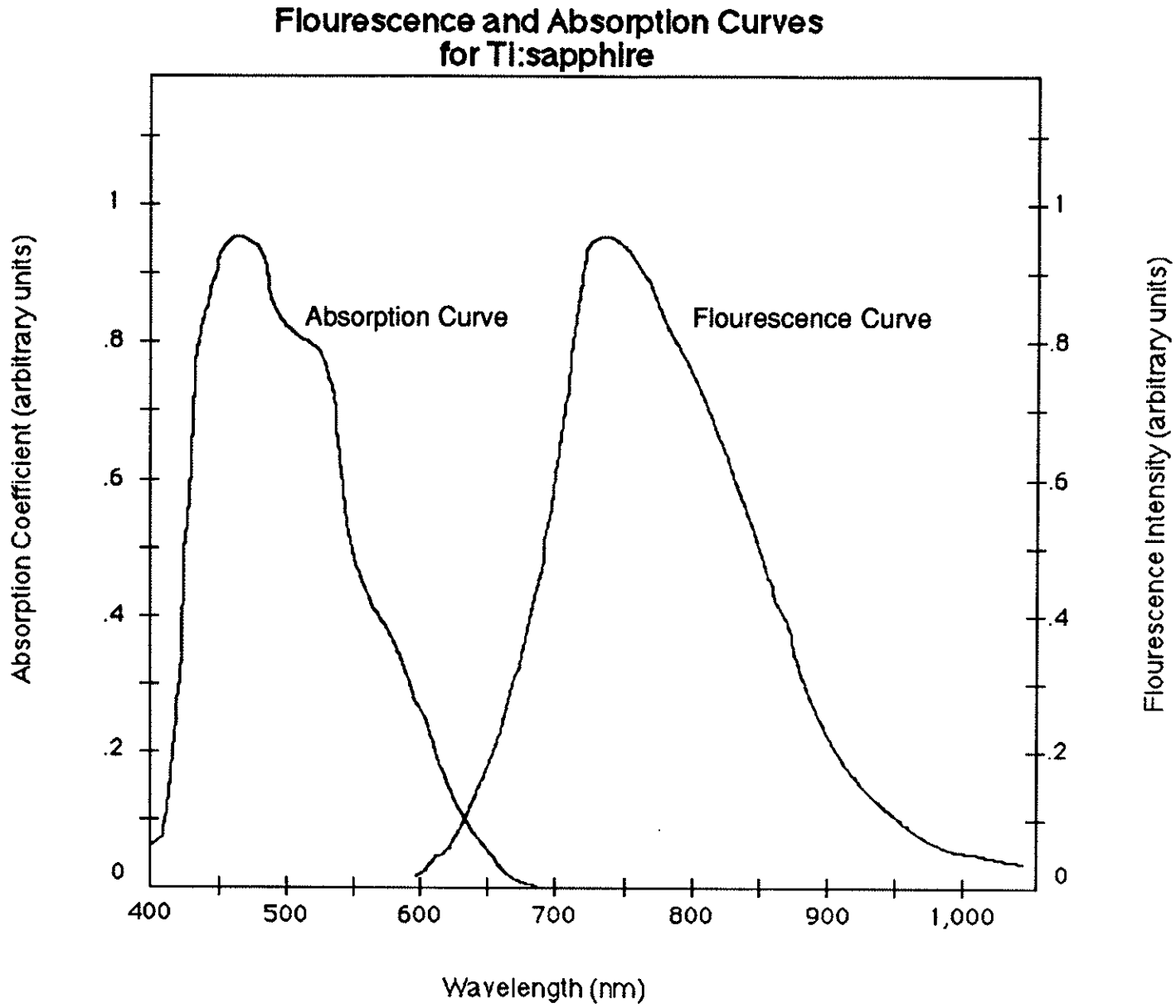
Flourescence and Absorption Curves
for Tl:sapphire
Absorption Coefficient (arbitrary units)
Flourescence Intensity (arbitrary units)
Absorption Curve
Flourescence Curve
0
.2
.4
.6
.8
1
400
500
600
700
800
900
1,000
Wavelength (nm)

Figure 1.

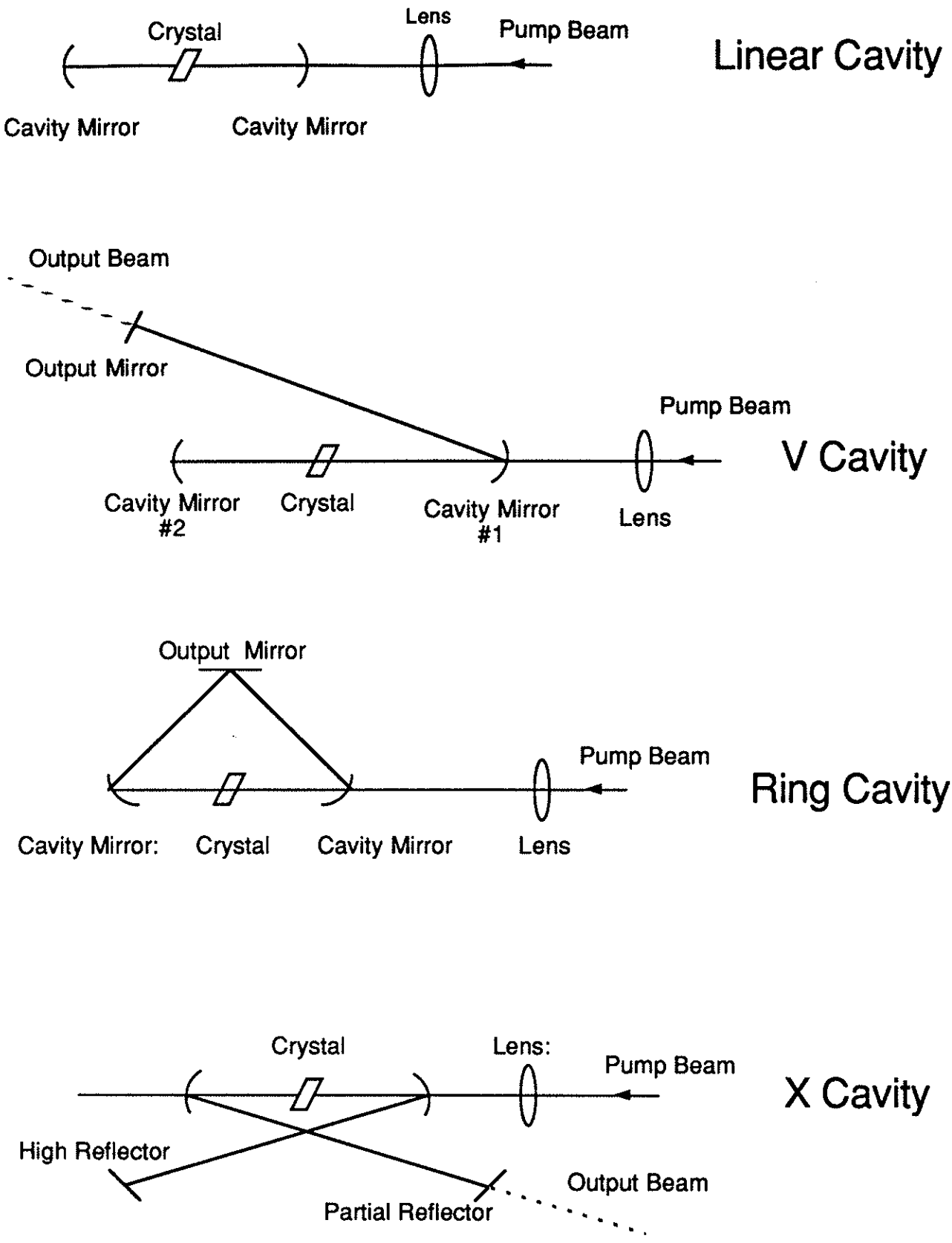
Crystal
Lens
Pump Beam
Linear Cavity
Cavity Mirror
Cavity Mirror
Output Beam
Output Mirror
Pump Beam
V Cavity
Cavity Mirror #2
Crystal
Cavity Mirror #1
Lens
Output Mirror
Pump Beam
Ring Cavity
Cavity Mirror:
Crystal
Cavity Mirror
Lens
Crystal
Lens:
Pump Beam
X Cavity
High Reflector
Output Beam
Partial Reflector

Figure 2.

Parts List

Quantity	Description	Source
1	Ti:sapphire crystal 4.75 mm path length, .15% doping, 5 mm height, 8 mm width	Union Carbide Crystal Products 750 S. 32nd Street Wahougal, Wa 98671 (206) 835-2001
2	10 cm radius of curvature mirrors, high reflector at 800 nm, high transmission at 488-514 nm part # G0079-012	Spectra-Physics Inc. Laser Products Division 1250 W. Middlefield Road P.O. Box 7013 Mountain View, Ca 94039-7013 (800) 456-2552
1	150 mm focal length, 25 mm diameter plano-convex lens part # M32,864	Edmund Scientific
1	longpass filter 1 in. diameter cut-off λ = 550 nm part # M32,764	Edmund Scientific
1	flat output coupler, 90% transmittance at 800 nm 1 in. diameter .125 in. thick part # PR2-800-90-1025	CVI West 361 Lindberg Avenue Livermore, CA 94550
1	prism table part # KM-B	Thor Labs P.O. Box 366 Newton, NJ. 07860 (201) 579-7227

Table 1.

Linear Cavity

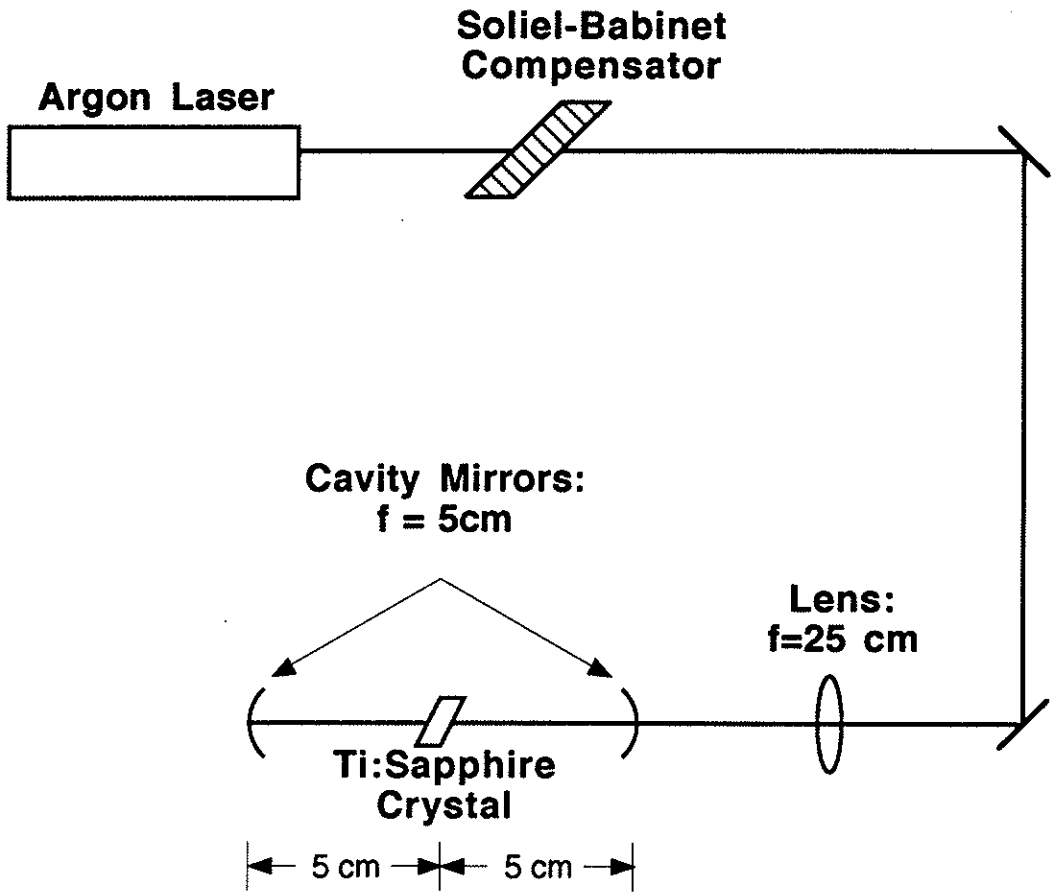

Figure 3.

Ring Cavity

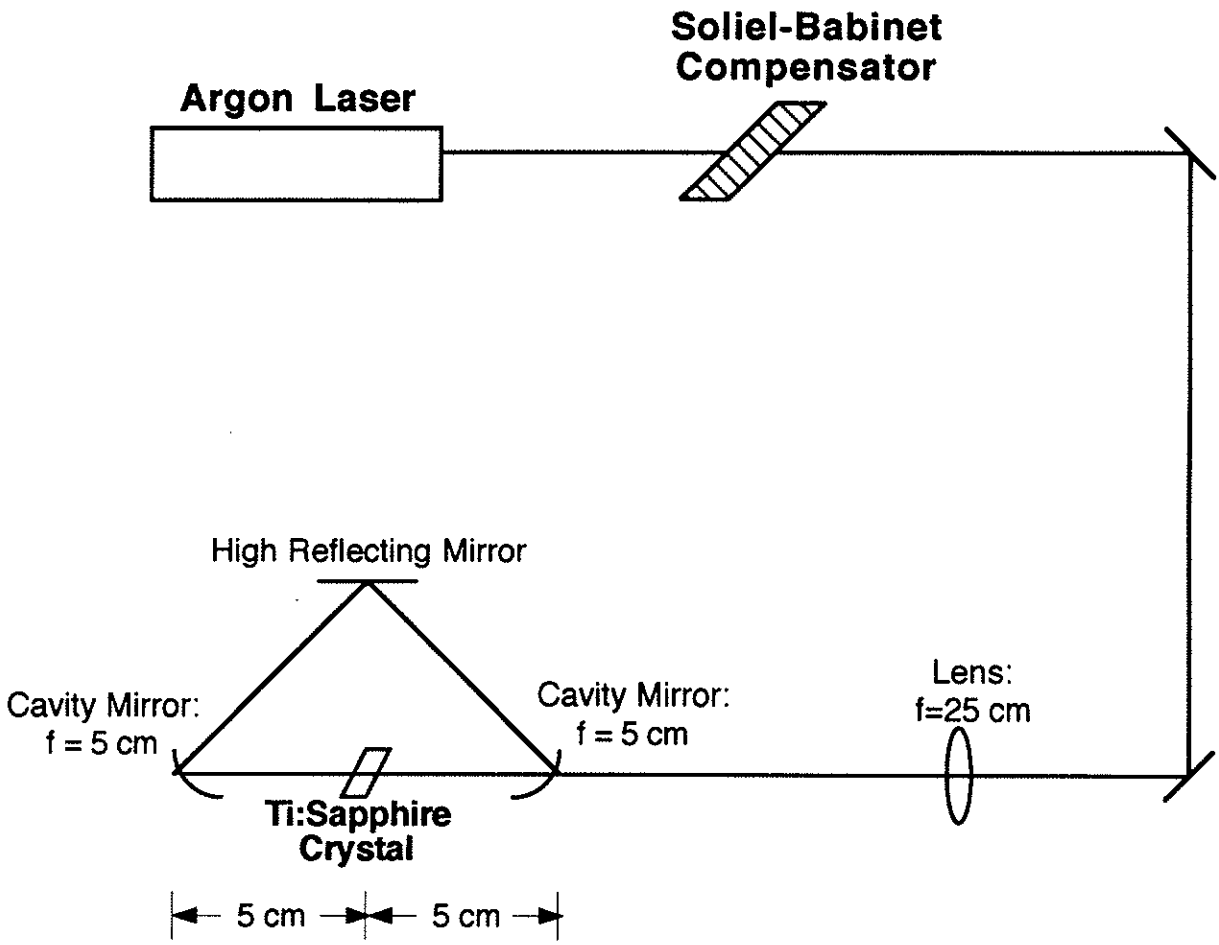

Figure 4.

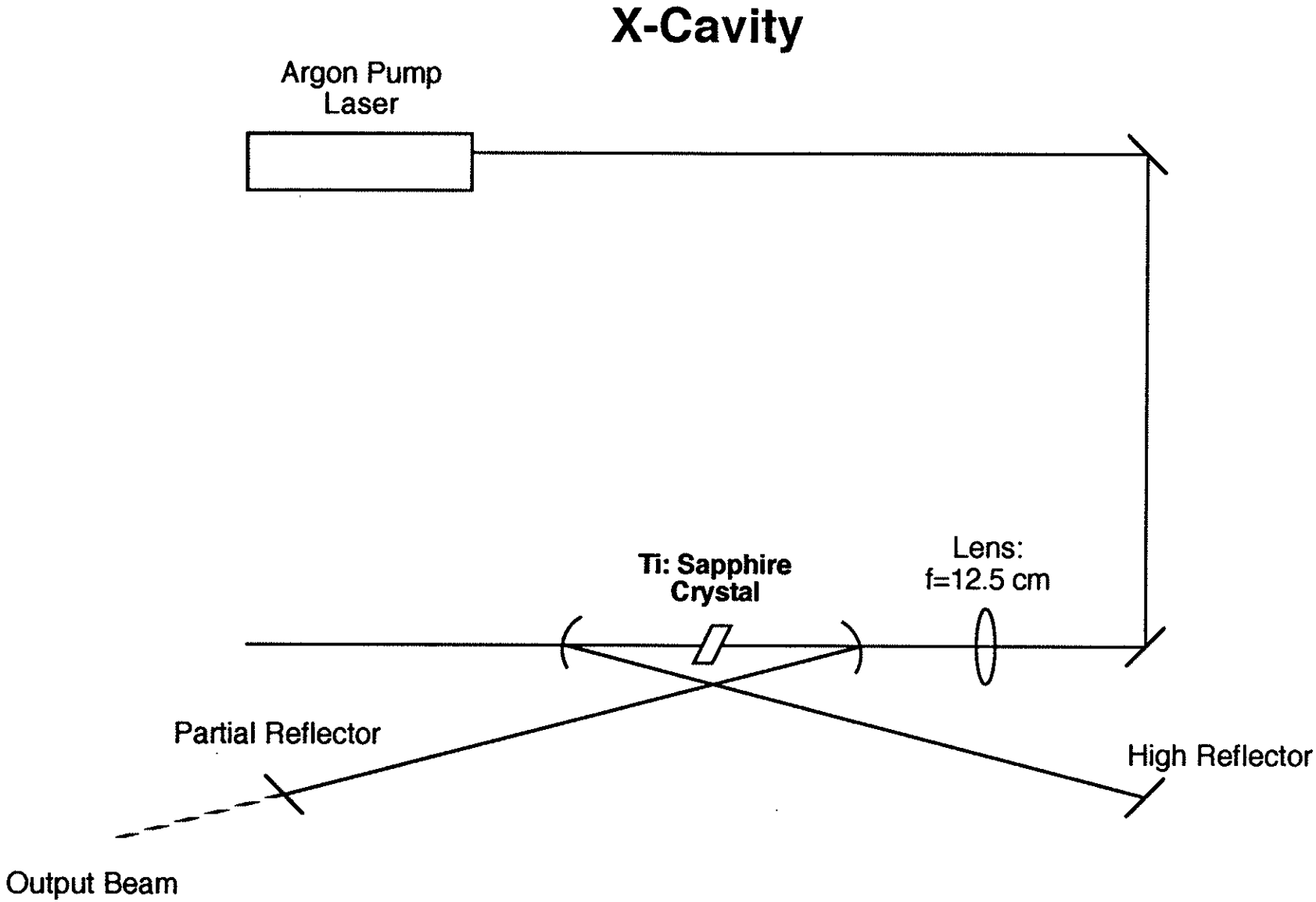
X-Cavity
Argon Pump
Laser
Ti: Sapphire
Crystal
Lens:
f=12.5 cm
Partial Reflector
High Reflector
Output Beam

Figure 5.

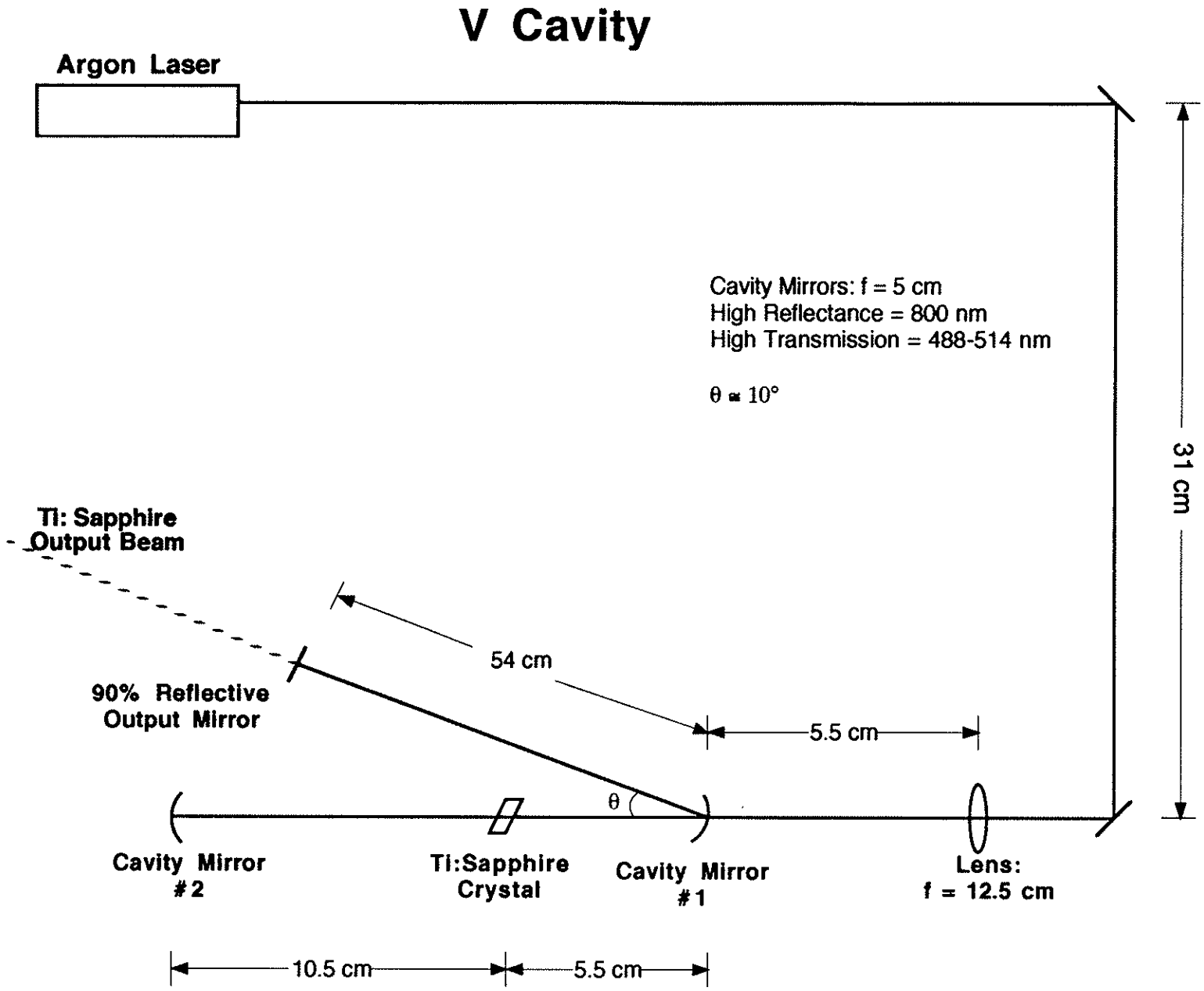
V Cavity
Argon Laser
Cavity Mirrors: f = 5 cm
High Reflectance = 800 nm
High Transmission = 488-514 nm
θ ≈ 10°
31 cm
Ti: Sapphire
Output Beam
54 cm
90% Reflective
Output Mirror
5.5 cm
θ
Cavity Mirror
#2
Ti:Sapphire
Crystal
Cavity Mirror
#1
Lens:
f = 12.5 cm
10.5 cm
5.5 cm

Figure 6.

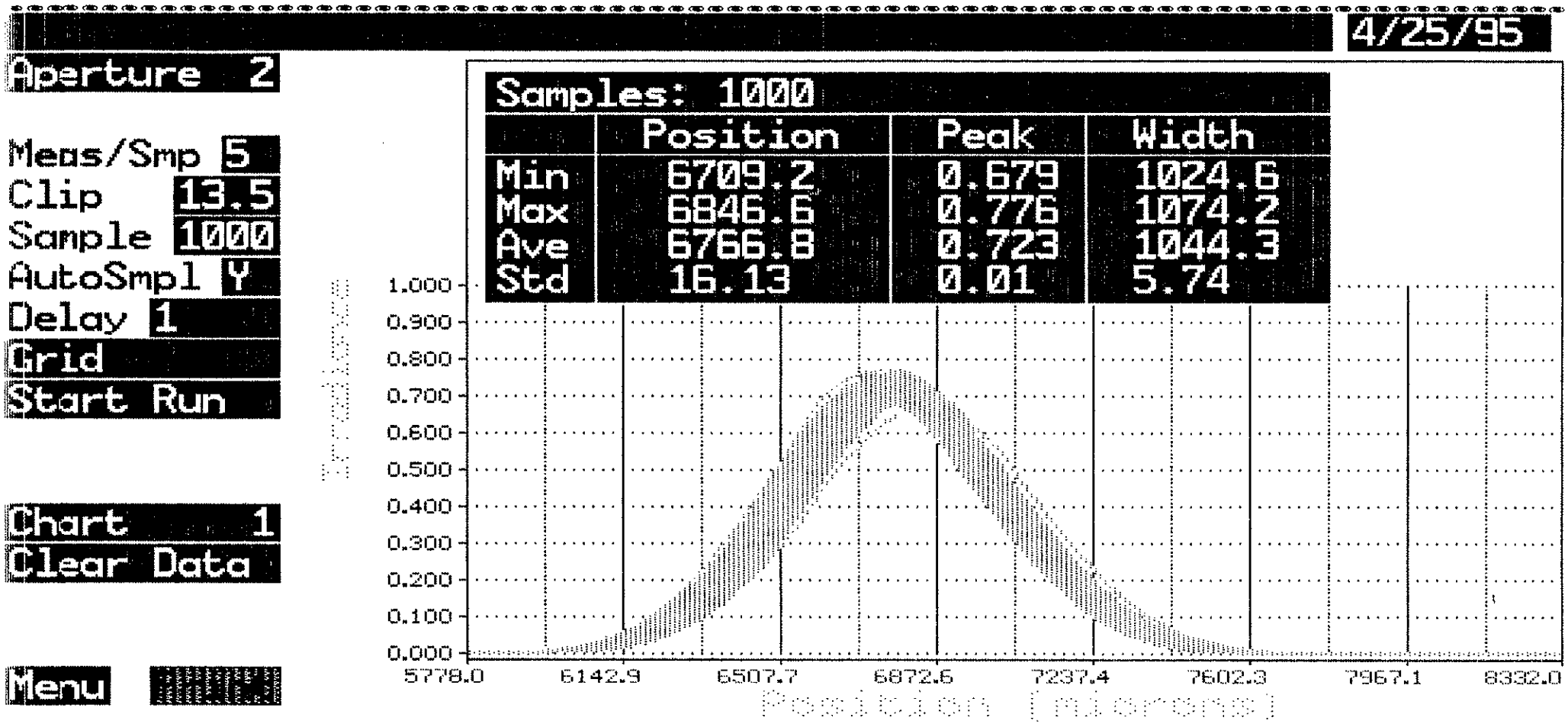
4/25/95
Aperture 2
Meas/Smp 5
Clip 13.5
Sample 1000
AutoSmpl Y
Delay 1
Grid
Start Run
Chart 1
Clear Data
Menu
Samples: 1000
Position
Peak
Width
Min 6709.2 0.679 1024.6
Max 6846.6 0.776 1074.2
Ave 6766.8 0.723 1044.3
Std 16.13 0.01 5.74
1.000
0.900
0.800
0.700
0.600
0.500
0.400
0.300
0.200
0.100
0.000
5778.0
6142.9
6507.7
6872.6
7237.4
7602.3
7967.1
8332.0

Figure 7.

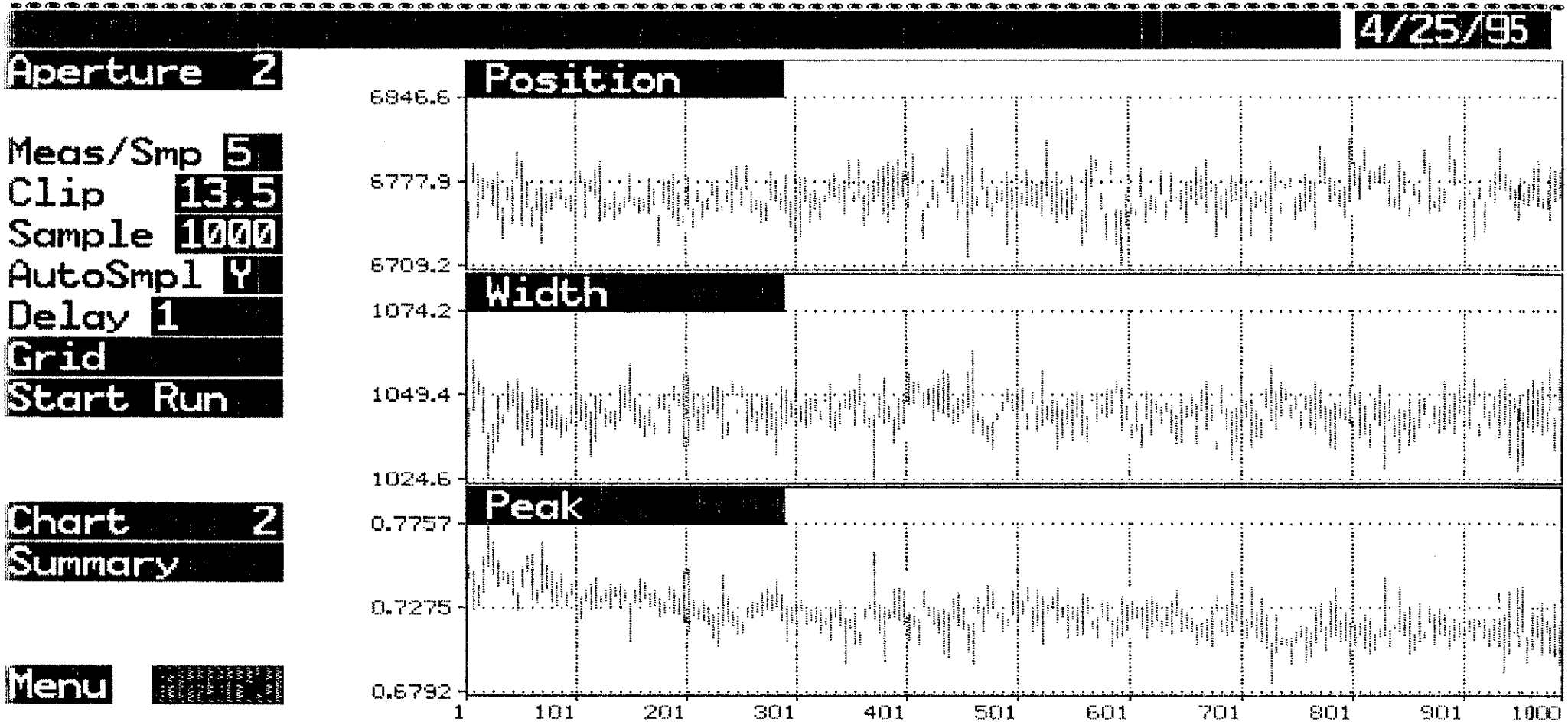
4/25/95
Aperture 2
Meas/Smp 5
Clip 13.5
Sample 1000
AutoSmpl Y
Delay 1
Grid
Start Run
Chart 2
Summary
Menu
Position
6846.6
6777.9
6709.2
Width
1074.2
1049.4
1024.6
Peak
0.7757
0.7275
0.6792
1
101
201
301
401
501
601
701
801
901
1000

Figure 8.

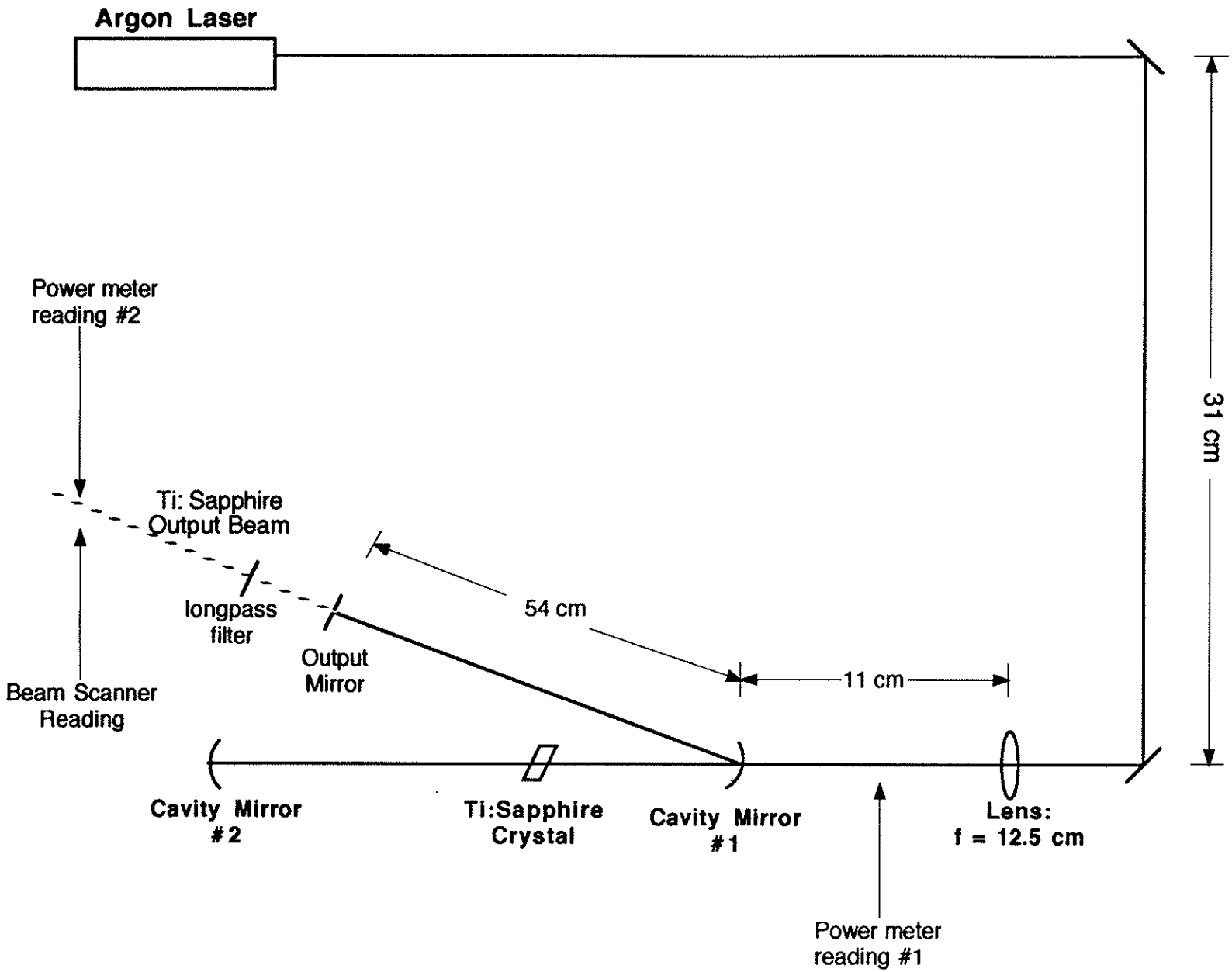
Argon Laser
Power meter
reading #2
Ti: Sapphire
Output Beam
longpass
filter
Output
Mirror
54 cm
11 cm
31 cm
Beam Scanner
Reading
Cavity Mirror
#2
Ti:Sapphire
Crystal
Cavity Mirror
#1
Lens:
f = 12.5 cm
Power meter
reading #1

Figure 9.

Figure 10.

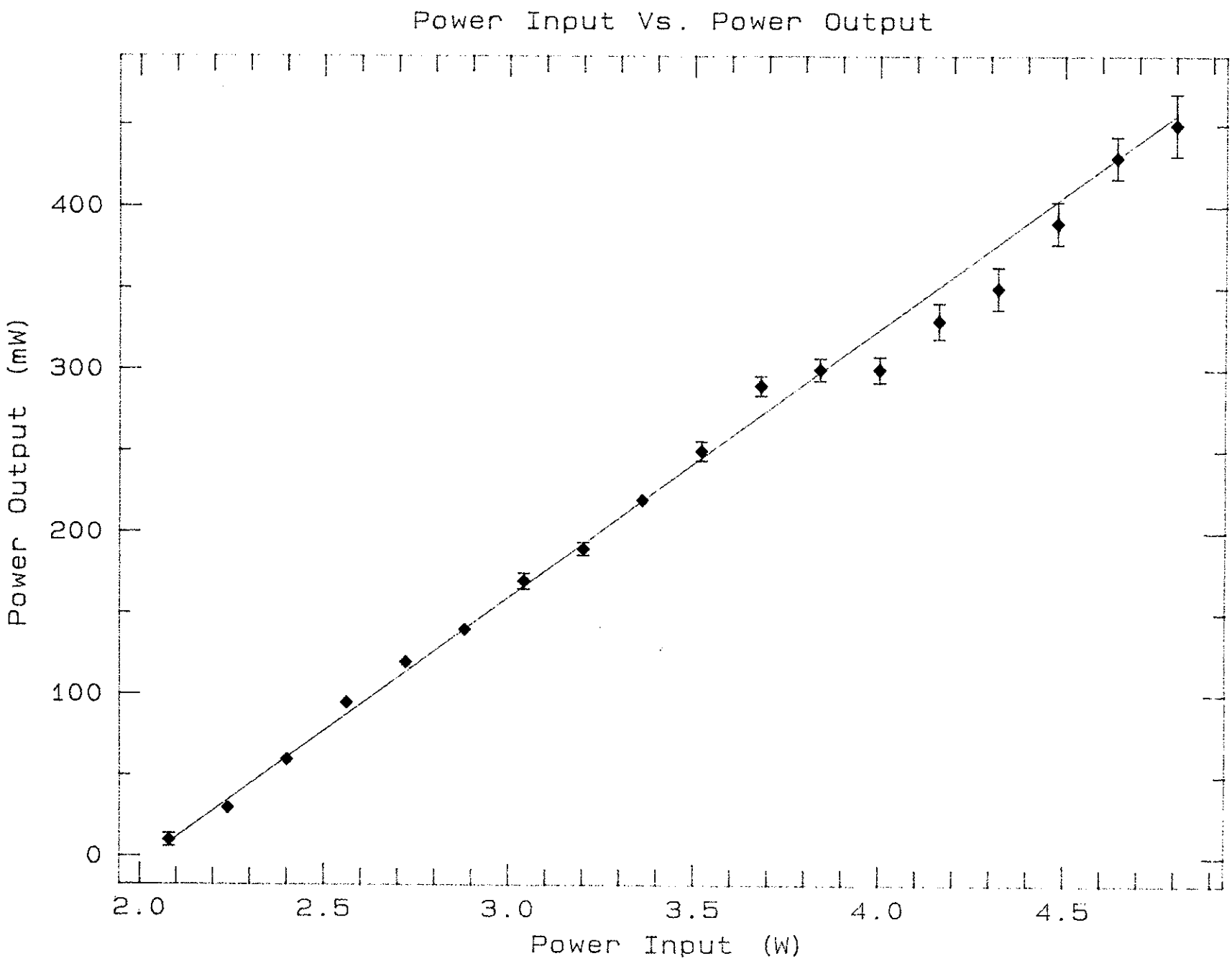
Power Input Vs. Power Output
Power Output (mW)
0
100
200
300
400
2.0
2.5
3.0
3.5
4.0
4.5
Power Input (W)

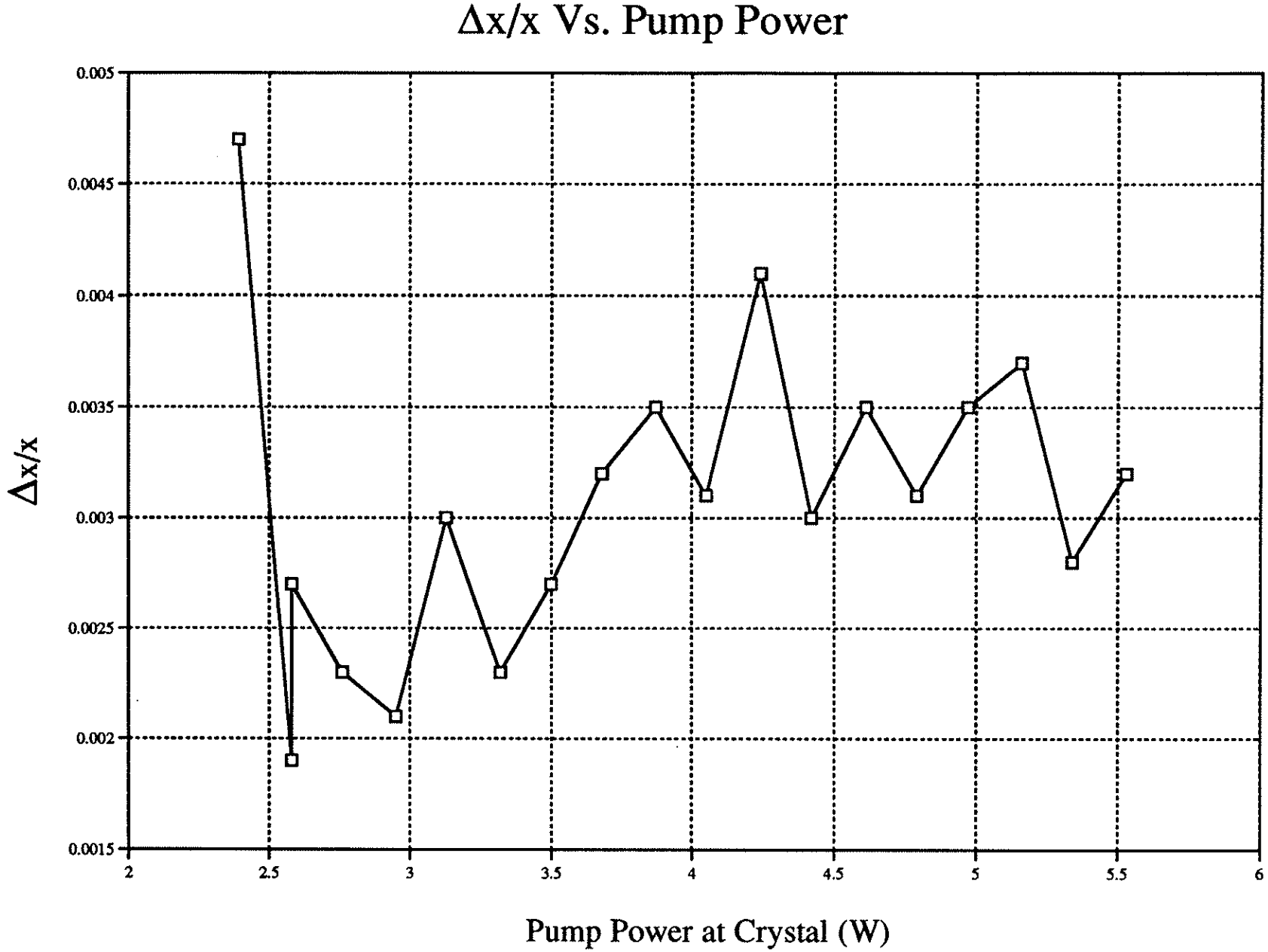
Δx/x Vs. Pump Power
0.005
0.0045
0.004
0.0035
0.003
0.0025
0.002
0.0015
Δx/x
2
2.5
3
3.5
4
4.5
5
5.5
6
Pump Power at Crystal (W)

Figure 11.

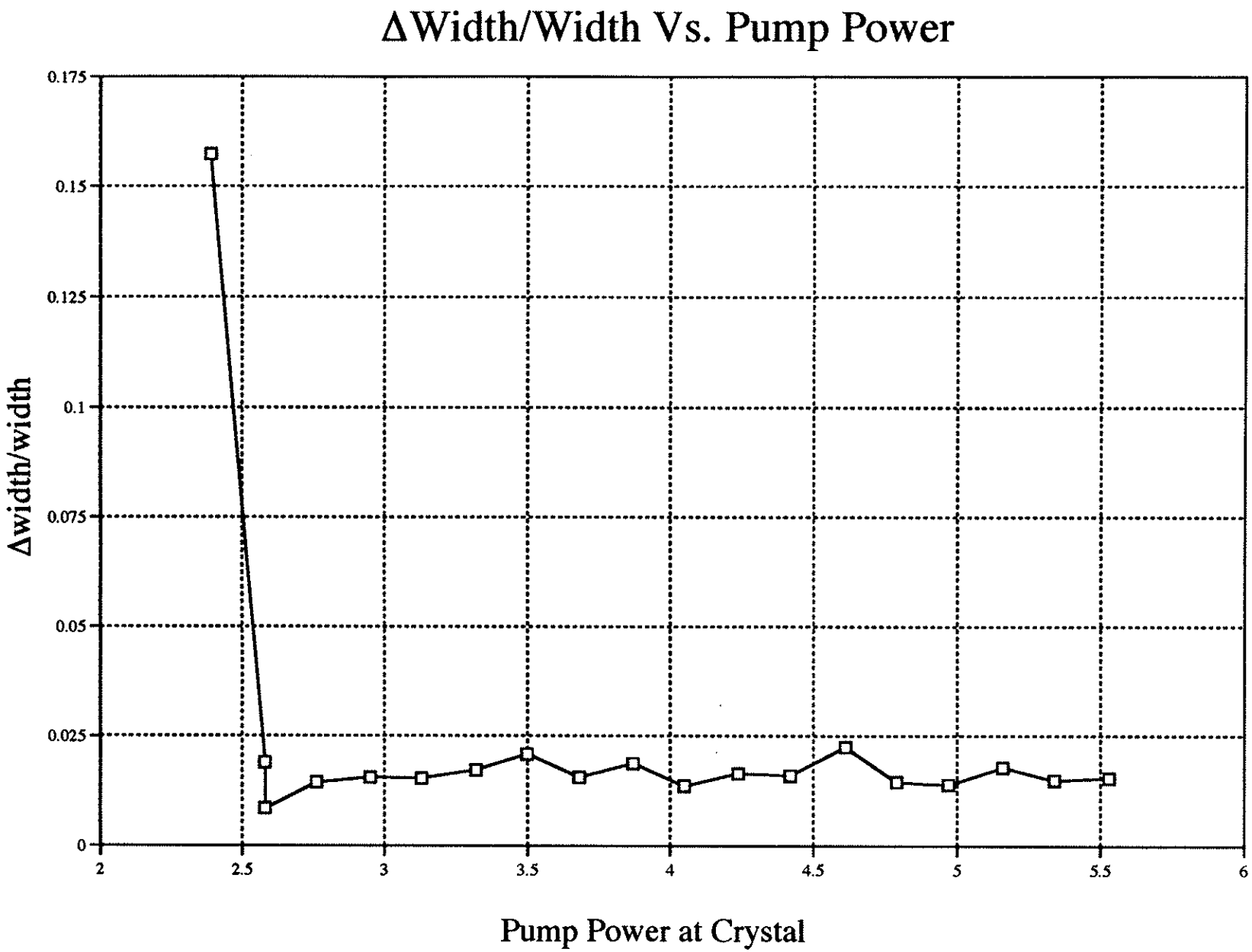
ΔWidth/Width Vs. Pump Power
Δwidth/width
0.175
0.15
0.125
0.1
0.075
0.05
0.025
0
2
2.5
3
3.5
4
4.5
5
5.5
6
Pump Power at Crystal

Figure 12.

Pump Power (W)	Power at Crystal (W)	Ti: Sapphire Power (mW)	Beam Position (μm)	Postion Standard Deviation	Beam Width (μm)	Width Standard Deviation
6	5.53	450	6423.8	20.82	1159.5	17.95
5.8	5.34	430	6414.3	18.03	1144.3	17.08
5.6	5.16	390	6430.8	23.84	1144.2	20.47
5.4	4.97	350	6442.3	22.84	1141.5	15.86
5.2	4.79	330	6441.3	20.23	1114.1	16.2
5	4.61	300	6455.4	22.53	1066.7	24.03
4.8	4.42	300	6467.4	19.24	1052.2	16.81
4.6	4.24	290	6470.8	26.32	1034.1	17.07
4.4	4.05	250	6474.2	20.31	1047.6	14.25
4.2	3.87	220	6479.7	22.88	1038.3	19.55
4	3.68	190	6479.3	20.74	1012.6	15.84
3.8	3.50	170	6484	17.42	1025	21.45
3.6	3.32	140	6490.9	14.95	1008.8	17.43
3.4	3.13	120	6497.8	19.62	1011	15.61
3.2	2.95	95	6495.8	13.96	1007.7	15.77
3	2.76	60	6499.7	15.14	1015.1	14.65
2.8	2.58	30	6511.1	12.19	1002.1	19.02
2.8	2.58	30	6394.4	17.36	1010.5	8.54
2.6	2.39	10	6403.5	29.88	1017.5	160.06

Table 2.

Power Before Lens (W)	Power At Crystal (W)	Power Adjustment
2.8	2.6	0.929
5.4	5	0.926
4.4	4	0.909

Power Before Crystal (W)	Power At Crystal (W)	Power After Crystal (W)	Crystal Absorbtion
5.2	5	1.1	0.780
4.4	4.2	1	0.762
3.4	3.2	0.75	0.766
4	3.8	0.8	0.789

Av. Power Adjustment
0.92

Av. Crystal Absorption.
77%

Table 3.